

# Active Vibration Suppression of a Nonlinear Flexible Spacecraft

M. Malekzadeh<sup>1</sup>

1. Department of Mechanical Engineering, University of Isfahan, Iran

Postal Code: 8174673441, Esfahan, IRAN

[m.malekzadeh@eng.ui.ac.ir](mailto:m.malekzadeh@eng.ui.ac.ir)

*In this article, the issue of attitude control and active vibration suppression of a nonlinear flexible spacecraft is assessed through piezoelectric patches as actuator and sensors. Two controller loops are applied: the inner loop, to make the panel vibration damped through piezoelectric patches; and the outer loop, to perform spacecraft maneuver using the reaction wheel acting on the hub. An optimal controller is designed in the inner loop and two robust controllers are designed as the outer loop, which are used interchangeably. One is a high-order sliding mode controller using super twisting algorithm and the other is a nonsingular terminal sliding mode controller. With respect to the non-minimum phase properties of the system, if the panel deflection is defined as the output, the output redefinition approach is introduced. The performances of the proposed controllers are compared in terms of tracking attitude trajectory, panel vibration suppression, robustness towards uncertainties, sensor noise, disturbances and nonlinearity in large maneuvers.*

**Keywords:** Active control, Flexible Spacecraft, piezoelectric patches, super twisting algorithm, nonsingular terminal sliding mode, output redefinition approach.

## Introduction

With respect to the complexity of a spacecraft in which large solar panels are used, the flexibility is a major requirement. Due to the large maneuver of the modern spacecraft, nonlinear controllers are used. Also, because of the existence of external disturbances, the sensors noises, and all the uncertainties, the design of a robust controller is a major concern.

One of the most common nonlinear robust methods is the sliding mode, labeled as the variable structure controller (VSC). The classic sliding modes (SM) provide robust and high-accuracy solutions to a wide range of control problems, but they are unable to remove the chattering effect [1].

Higher-order sliding modes (HOSM) act on the higher-order time derivatives of the sliding mode. The main advantages of the basic method are retained while the chattering effect is reduced and the accuracy is improved.

One of the most widely used high-order sliding mode algorithms, the super twisting algorithm (STA), can be applied in lieu of the classic sliding mode using the same information available [1]. It is proved that the STA improves the controller robustness while decreases the chattering effect [2, 3]. The stability and performance of STA on a quad-rotor is proved through Lyapunov functions [4-5]. In this article, an STA controller is designed for a flexible spacecraft.

Another issue, raised by designing other methods of sliding mode controllers, is the undesirable and improper functionality of the sliding mode controllers in complex dynamic systems. The terminal sliding mode controller has the following advantages:

1. Ensuring the system convergence in a limited time in a complex system
2. Providing fast and accurate response according to the definition of nonlinear sliding surfaces bounded
3. Enjoying an easier implementation compared with all other extended SMCS due to its simple sliding surface and controlling rule.

---

1. Assistant Professor (Corresponding Author)

The biggest drawback of this control method is revealed when the target is located around singular points. In such an area, the non-singular terminal sliding mode controllers are used.

The terminal sliding mode controllers have several applications: applying non-singular terminal controller on the flexible robotic arms [6], the missiles navigation systems [7], the direct current convertor [8] and the second fractional order nonlinear systems [9]. In this article, nonsingular terminal-sliding mode controller is designed for the flexible spacecraft.

Over the last decades, the application of smart materials as actuators and sensors has increased considerably and this provides effective means for high quality actuation and sensing mechanism. The piezoelectrics are known as: low-cost, light weight, low power consumption and easy-to-implement materials for the active control of structure vibration [10]. A wide range of approaches are proposed in using piezoelectric material to actively control the vibration of flexible structures like: strain rate feedback control [11], positive position feedback (PPF) [12], modal velocity feedback [13], and linear quadratic regulator control [14-15]. It is observed that LQG control provides damping to all vibration modes of the spacecraft panel; however, it cannot provide high damping for a specific vibration mode.

In this article, LQG controller is applied in damping panel vibration of flexible spacecraft. In active flexible spacecraft control, three methods have been adapted in the previous studies:

In the first method, the system is described through angular attitude and panel deflection as the state vector. The reaction wheels torques and piezo electric voltages are used as the control inputs. The controller is designed based on this defined state space form. In this method, designed controller is complex. According to [16], an adaptive neural network is used to control the spacecraft attitude and panel vibration.

In the second method, considering small perturbation, the flexible spacecraft dynamic equation is separated in order to allow for two separate controller designs: one for controlling the central rigid hub and the other for controlling the panel vibration. However, this method is weak in its performance in the large maneuver because some coupling terms are ignored in the dynamic equation. Optimal controller is used to track attitude angle, and PPF method is used to damp panel vibration [17]. Also the sliding mode and inverse dynamic methods are applied in controlling

Euler angles, and Lyapunov method is applied in damping the panel vibration in [18].

In the third method, two inner and outer controller loops are used. The inner loop is used in controlling panel vibration and the outer loop controls the spacecraft attitude with the assumption that the spacecraft attitude has no effect on the inner loop and it is considered equal to zero. Hence, a separate deflection equation is achieved without any spacecraft attitude state. According to [19], adaptive controller is used as the outer loop and PPF is used as inner loop controller. In this study, the third method is used.

Here, first the two passive controllers using STA and the nonsingular terminal SMC are introduced. Because of non-minimum phase properties of the flexible spacecraft dynamic, while panel deflection is considered as output, the output is redefined and controller is designed based on this new output. Second, two active controllers are designed by considering the STA and nonsingular terminal sliding mode controllers; as this outer loop controller acts on the reaction wheel, and the LQG method as the inner loop acts on piezoelectric patches. The performance of the proposed controllers is compared in combined uncertain condition (in the presence of disturbance, sensor noise and plant uncertainties) considering actuators saturation.

### Flexible Spacecraft Equations

The flexible spacecraft considered consists of a rigid hub and N appendages and  $n_p$  piezoelectric patches attached to it. Each panel with the density,  $\rho_{bi}$ , length,  $l_i$ , is attached to the hub from a distance,  $b_i$  (Figure 1).

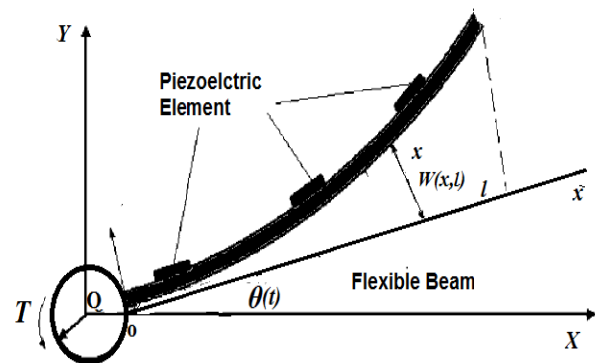


Figure 1. Flexible spacecraft model

The total kinetic energy is composed of the kinetic energies of the hub ( $T_h$ ), the appendages

( $T_i$ ), and piezoelectric patches ( $T_p$ ) can be written as [20]:

$$T = \frac{1}{2} \omega^T I_h \omega + \sum_{i=1}^N T_i + \sum_{i=1}^{n_p} T_{pi}, \quad (1)$$

$$T_i = \frac{1}{2} \int_0^l \rho_{bi} V_i^T V_i dx = \int_0^l \rho_{bi} (b + x)^2 \dot{\theta}^2 + 2(b+x)\dot{\theta}\dot{y} + \dot{y}^2 + y^2 \dot{\theta}^2 dx \quad (2)$$

$$T_{pi} = \frac{1}{2} \int_{x_i}^{h_i+x_i} \rho_{pi} V_i^T V_i dx \quad (3)$$

Where  $I_h$ ,  $\omega$ , and  $V_i$  are the hub inertia moment, spacecraft angular velocity, and the panel velocity, respectively.  $\rho_{pi}$ ,  $x_i$ , and  $h_i$  are the mass per unit length, starting x-coordinate and length of  $i^{\text{th}}$  PZT patch, respectively.

To model the vibration of the flexible appendages, the assumed modes formulation is used. The panel deflection along the body axis is written as:

$$w_i = w_i(y, t) = \sum_{i=1}^n q_i(t) \varphi_i(y) = \varphi_i q_i \quad (4)$$

$n$  is the number of assumed modes.  $q_i$  and  $\varphi_i$  are the modal coordinates and the panel shape functions, respectively. The mode shape functions of the clamped-free beams,  $\varphi_s(y)$ , can be written as:

$$\varphi_s(y) = \left\{ \left[ \cosh(\lambda_s \frac{y}{l}) - \cos(\lambda_s \frac{y}{l}) \right] - \sigma_s \left[ \sinh(\lambda_s \frac{y}{l}) - \sin(\lambda_s \frac{y}{l}) \right] \right\} \quad (5)$$

$$\sigma_s = \frac{\sinh(\lambda_s) - \sin(\lambda_s)}{\cosh(\lambda_s) + \cos(\lambda_s)} \quad (6)$$

Where  $\lambda_s$  is root of the following equation:

$$\cosh(\lambda_s) + \cos(\lambda_s) + 1 = 0 \quad (7)$$

The potential energy of panel deformation is given as:

$$P = \sum_{i=1}^N \int E_i I_i y_i''^2 dy = \sum_{i=1}^N \frac{E_i t_i^3}{12} \int q_i^T \varphi_i''^T \varphi_i'' q_i dy \quad (8)$$

Where  $t_i$  and  $E_i$  are the thickness and elasticity modulus of the  $i^{\text{th}}$  appendage, respectively.

The one-dimensional electro-mechanical constitutive equation of a piezoelectric element by assuming uniaxial polarized and homogeneous layers can be written as:

$$\begin{bmatrix} D_3 \\ S_1 \end{bmatrix} = \begin{bmatrix} \varepsilon_3^T & d_{31} \\ d_{31} & S_{11}^E \end{bmatrix} \begin{bmatrix} E_3 \\ T_1 \end{bmatrix} \quad (9)$$

where  $D_3$ ,  $S_1$ ,  $E_3$ ,  $T_1$ ,  $d_{ij}$  and  $S_{ij}^E$  represent the electric displacement along the  $i^{\text{th}}$  axis,

permittivity of the piezoelectric material, the electric field density, piezoelectric charge, and elastic constants of the piezoelectric materials, respectively [10].

According to the fact that in the piezo material, the Young's modulus  $E_p$ , is the inverse of its elastic constant  $S_{11}^E$ , equation (9) can be written as:

$$\begin{bmatrix} D_3 \\ T_1 \end{bmatrix} = \begin{bmatrix} \varepsilon_3^T - d_{31} E_p & d_{31} E_p \\ -d_{31} E_p & E_p \end{bmatrix} \begin{bmatrix} E_3 \\ S_1 \end{bmatrix} \quad (10)$$

The work done by the  $i^{\text{th}}$  PZT patches is defined as an integral over the volume of the PZT patches such that:

$$W_{pi} = \frac{1}{2} \int_{V_i} (-T_i S_{1i} + D_{3i} E_{3i}) dv_i = \frac{1}{2} w_{pi} \int_{x_i}^{h_i+x_i} \int_{y_i}^{y_i+t_i} \begin{Bmatrix} D_{3i} \\ T_i \end{Bmatrix} \begin{bmatrix} 1 & 0 \\ 0 & -1 \end{bmatrix} \begin{Bmatrix} E_{3i} \\ S_{1i} \end{Bmatrix} dv \quad (11)$$

where  $y_i$  is the starting point of piezoelectric as measured from the neutral axis of the beam.  $v_i$  and  $w_{pi}$  are the electrode voltage and the width of the  $i^{\text{th}}$  piezo patch, respectively. Using the Lagrange's equation, we have:

$$\begin{bmatrix} J + q^T [M] q & [\tilde{\varphi}] \\ [\tilde{\varphi}] & [M] \end{bmatrix} \begin{bmatrix} \dot{\theta} \\ \dot{q} \end{bmatrix} + \begin{bmatrix} 0 & 0 \\ 0 & [K] - \dot{\theta}^2 [M] \end{bmatrix} \begin{bmatrix} \theta \\ q \end{bmatrix} + \begin{bmatrix} 2 \dot{\theta} q^T [M] q \\ 0 \end{bmatrix} = \begin{bmatrix} \tau \\ -[B]v \end{bmatrix} \quad (12)$$

$$J = I_h + \int_0^l \rho_b (b+x)^2 dx + \sum_{i=1}^{n_p} \int_{x_i}^{h_i+x_i} \rho_{pi} (b+x)^2 dx \quad (13)$$

$$[M] = \int_0^l \rho_b \{\varphi\}^T \{\varphi\} dx + \sum_{i=1}^{n_p} \int_{x_i}^{h_i+x_i} \rho_{pi} \{\varphi\}^T \{\varphi\} dx \quad (14)$$

$$[\tilde{\varphi}] = \int_0^l \rho_b (b+x) \{\varphi\} dx + \sum_{i=1}^{n_p} \int_{x_i}^{h_i+x_i} \rho_{pi} (b+x) \{\varphi\} dx \quad (15)$$

$$[K] = [K_b] + [K_{pi}] = \int_0^l E_b I_b \{\varphi''\}^T \{\varphi''\} dx + w_{pi} t_{pi} E_p \left( y_i^2 + y_i t_{pi} + \frac{t_{pi}^2}{3} \right) \int_{x_i}^{h_i+x_i} \{\varphi''\}^T \{\varphi''\} dx \quad (16)$$

$$[B_i] = d_{31} E_p w_{pi} \left( y_i + \frac{t_{pi}}{2} \right) \int_{x_i}^{h_i+x_i} \{\varphi''\}^T dx \quad (17)$$

## Active Control Strategies Applying Piezoelectric Patches

The control system for the vibration reduction of the flexible spacecraft during attitude maneuvering consists of the two independent subsystems shown in Figure 2. The inner active controller can suppress the vibration and the outer spacecraft attitude controller guarantees the system stability and performance [19].

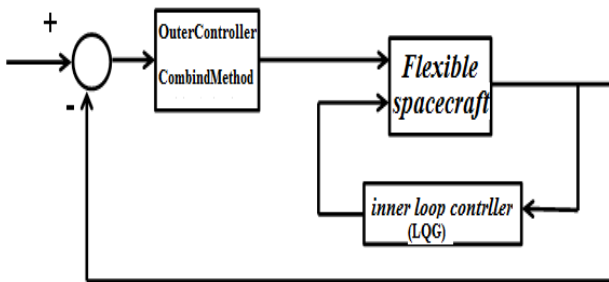


Figure 2. Block diagram of control system with piezoelectric

### Inner loop control strategy

It is assumed that spacecraft orientation has no effect in the inner loop. For active vibration control of the flexible appendage, an LQR controller is designed using piezoelectric actuators and sensors. Three piezo patches are used on the spacecraft panel: attached at the root, in the middle and at the end of the panel.

The objective is designing inner loop optimal controller to dampen the panel vibration. By considering  $\dot{\theta} = \ddot{\theta} \cong 0$ , the elastic vibration dynamics become decoupled from the rigid body motion dynamics. By imposing this condition, equation (12) becomes:

$$[M]\ddot{q} + [K]q = -B v \quad (18)$$

In this equation, by choosing the state vector  $X = \begin{bmatrix} \dot{q} \\ q \end{bmatrix}$ , the state space equation can be expressed as:

$$\dot{X} = \begin{bmatrix} 0 & -M^{-1}K \\ I & 0 \end{bmatrix} X + \begin{bmatrix} -B \\ 0 \end{bmatrix} v \quad (19)$$

In optimal control problem, the state feedback gain matrix  $K$  is designed in a manner that the quadratic integral criterion  $J = \int_0^\infty [X^T Q X + U^T R U] dt$  is minimized. The weighting matrixes  $Q$  and  $R$  are positive definite matrixes that penalize certain states and control inputs of the

system. The solution to this problem is provided by the following feedback control law:

$$U = -KX(t) = -R^{-1}B^T P(t)X(t) \quad (20)$$

Where,  $P(t)$  is extracted by solving the following Riccati equation:

$$A^T P + PA - PBR^{-1}B^T P + Q = 0 \quad (21)$$

By changing the weight of  $Q$  and  $R$  and selecting their best,  $K$  can be achieved optimally.

### Outer loop control strategy

After vibration suppression compensator is designed, the second feedback loop is designed to guaranty the maneuver of the flexible spacecraft. The equations of motion for the flexible spacecraft without piezoelectric voltage are given in (22), with the same mass as described by equation (12):

$$\begin{bmatrix} J + q^T [M] q & [\tilde{\varphi}] \\ [\tilde{\varphi}] & [M] \end{bmatrix} \begin{bmatrix} \ddot{\theta} \\ \ddot{q} \end{bmatrix} + \begin{bmatrix} 0 & 0 \\ 0 & [K] - \dot{\theta}^2 [M] \end{bmatrix} \begin{bmatrix} \theta \\ q \end{bmatrix} + \begin{bmatrix} 2 \dot{\theta} q^T [M] q \\ 0 \end{bmatrix} = \begin{bmatrix} \tau \\ 0 \end{bmatrix} \quad (22)$$

Two robust variable structure nonlinear controllers are designed as the outer loop: the high order-sliding mode, using super twisting algorithm and the nonsingular terminal sliding mode. For a better comparison of the performance of active and passive controllers, they are designed in a manner that the piezo actuators output is not involved.

## High Order Sliding Mode Controller, STA

The objective is to control the attitude angle and panel deflection of the flexible spacecraft. The Euler angle  $\theta$  represents the spacecraft angular attitude obtained from the body frame respected to the inertial frame:

In this section, using Super Twisting Algorithm (STA), a robust controller is designed for the flexible spacecraft. The tracking of the attitude angles  $\theta$  to the command trajectory  $\theta_d$  and damping panel deflection are the main objective.

Using the state vector  $X = [x_1 \ x_2] = [\theta \ q]$  and (22), the state-space equation of the flexible spacecraft model can be obtained as:

$$\begin{cases} \dot{x}_1 = x_1 \\ x_2 = f(X) + g(X)u + d(t) \end{cases} \quad (23)$$

$$f(X) = \begin{bmatrix} J + q^T[M]q & [\tilde{\varphi}] \\ [\tilde{\varphi}] & [M] \end{bmatrix}^{-1} \begin{bmatrix} 0 & 0 \\ 0 & [K] - \dot{\theta}^2[M] \end{bmatrix} \begin{bmatrix} \theta \\ q \end{bmatrix} + \begin{bmatrix} 2\dot{\theta}q^T[M]q \\ 0 \end{bmatrix} \quad (24)$$

$$g(X) = \begin{bmatrix} J + q^T[M]q & [\tilde{\varphi}] \\ [\tilde{\varphi}] & [M] \end{bmatrix}^{-1} \begin{bmatrix} 1 \\ 0 \end{bmatrix} \quad (25)$$

Where,  $d(t)$  is the disturbance vector. The functions  $f(X)$  and  $g(X)$  are not exactly known, but are bounded by a known continuous function of  $X$ .

If the panel deflection is assumed as output, the flexible spacecraft dynamics is non-minimum phase, then the spacecraft can be hardly controlled using panel deflection feedback. For getting the ability of controlling the spacecraft attitude, while damping panel deflection using only the reaction wheel actuator on the hub, the new output should be redefined composed of the two states as:

$$y = \theta + \alpha q \quad (26)$$

Where  $0 < \alpha < 1$ . As  $\alpha$  value increases, damping deflection is more important. Using equation (23-25), we can write:

$$\ddot{y} = A_1 + A_2 \tau \quad (27)$$

$$A_1 = f_2 + \alpha f_4 \quad (28)$$

$$A_2 = g_2 + \alpha g_4 \quad (29)$$

Taking  $X_1 = \theta + \alpha q$  and  $X_2 = \dot{\theta} + \alpha \dot{q}$ , From equation (27), we can write:

$$\dot{X}_1 = X_2 \quad (30)$$

$$\dot{X}_2 = \ddot{\theta} + \alpha \ddot{q} = (f_2 + \alpha f_4) + (g_2 + \alpha g_4)\tau \quad (31)$$

Hence, we have:

$$\dot{X} = f_S(X) + g_S(X)\tau \quad (32)$$

$$f_S = \begin{bmatrix} \dot{\theta} + \alpha \dot{q} \\ (f_2 + \alpha f_4) \end{bmatrix}$$

$$g_S = \begin{bmatrix} 0 \\ (g_2 + \alpha g_4) \end{bmatrix}$$

The control law will be introduced to converge in the states  $X_i$ , to the corresponding desired trajectories  $X_i^d$ . For this purpose, the following assumptions are of concern [21]:

1. The signals  $X_1$  can be measured by sensors
2. The command trajectories and their first and second time derivatives are bounded
3. The control signals (input to the spacecraft actuators) are bounded because of the power and saturation of the actuators

According to these assumptions and Eq. (23), the disturbances should be bounded as well, that is:

$$|d_i(t)| \leq \delta_i \quad (i = 1, 2, 3) \quad (33)$$

The main objective here is to execute the sliding mode on the following surface [21]:

$$s = \dot{e} + \lambda e \quad (34)$$

where,  $e = X_1 - X_1^d$ ,  $\dot{e} = X_2 - X_2^d = \dot{X}_1 - \dot{X}_1^d$  and  $\lambda = \text{diag}[\lambda_1, \lambda_2, \lambda_3]$  is a diagonal positive definite matrix. The stability and convergence of  $s$  and  $\dot{s}$  into zero should be assessed. The sliding surface is proposed as [21-22]:

$$\dot{s}_i = -k_{1i}|s_i|^{0.5} \text{sign}(s_i) - k_{2i} \int_0^t \text{sign}(s_i(\tau)) d\tau \quad (35)$$

Where, the following new variables are defined as:

$$z_{1i} = s_i$$

$$z_{2i} = -k_{2i} \int_0^t \text{sign}(s_i(\tau)) d\tau + w_i(t) \quad (i = 1, 2, 3)$$

$$w_i = \rho_i(t) \quad (36)$$

By applying Eq. (34), Eq. (36) can be rewritten as in[1]:

$$\dot{z}_{1i} = -k_{1i}|z_{1i}|^{\frac{1}{2}} \text{sign}(z_{1i}) + z_{2i}$$

$$\dot{z}_{2i} = -k_{2i} \text{sign}(z_{1i}) + \rho_i(t) \quad (i = 1, 2, 3) \quad (37)$$

Eq.(37) is the standard form of STA. The chosen Lyapunov function is presented as follows [22]:

$$V = \zeta^T P \zeta$$

$$\zeta = \left[ |z_1|^{\frac{1}{2}} \text{sign}(z_1) z_2 \right]^T = [\zeta_1 \quad \zeta_2] \quad (38)$$

The following controller is proposed by[1]:

$$u = g^{-1} \left( \dot{x}_1^d - \lambda \dot{e} - K_1 |s|^{\frac{1}{2}} \text{sign}(s) - \right.$$

$$\left. K_2 \int_0^t \text{sign}(s(\tau)) d\tau - f(x) \right) \quad (39)$$

Applying the Lyapunov stability theorem, the finite time zero convergence of variables  $z_{1i}$  and  $z_{2i}$  with the controller (39), is approved [22]. It follows that if the conditions on the gains given by Eq. (40) are met,  $s_i$  approaches zero in finite time,  $\lim_{t \rightarrow \infty} e = 0$ .

By applying Lyapunov stability theorem, the gains  $k_{1i}$  and  $k_{2i}$  ( $i = 1, 2, 3$ ) should be chosen according to the following relations:

$$k_{2i} > \delta_i$$

$$k_{1i}^2 > 4k_{2i} i = 1, 2, 3 \quad (40)$$

Hence, the gains can be constructed through  $\delta$ .

If  $\delta$  would be the environment disturbance, from (27), we can write:

$$\dot{X}_2 = A_1 + A_2(\tau + \delta) \quad (41)$$

As shown in (41),  $A_2 \delta$  acts as term  $d(t)$  to (23).

By considering uncertainty on the parameters such as  $I_c$ , (27) can be rewritten as:

$$\dot{X}_2 = (A_2 + \Delta A_2) \tau + (A_1 + \Delta A_1) =$$

$$A_2 \tau + A_1 + \Delta A_2 \tau + \Delta A_1 \quad (42)$$

Hence using (40 -41) the  $d$  in (23), can be represented as:

$$d = A_2 \delta + \Delta A_2 \tau + \Delta A_1 \quad (43)$$

In the simulations, the environment disturbances are modeled as the following equation:

$$\tau_d = \left[ 0.005 - 0.05 \sin\left(\frac{2\pi t}{400}\right) + \right. \quad (44)$$

$$\left. \delta(200, 0.2) + v_1 \right] (N.m)$$

Where  $\delta(T, \Delta T)$  and  $v_1, v_2$  and  $v_3$  denote an impulsive disturbance (magnitude 1, period  $T$ , and width  $\Delta T$ ) and white Gaussian noises (mean values of 0 and variances of  $0.005^2$ ), respectively. The uncertainty on the parameter of  $J$  in (22) is assumed up to 20%. The state vectors and controller effort are bounded as:

$$|X_{1i}| < \frac{\pi}{2} |X_{2i}| < 0.05 \text{ rad/s} \quad |u| <$$

$$0.8 \text{ N.m} \quad |\dot{u}| < 0.8 \text{ N.m/s} \quad (45)$$

According to (45), the  $\delta$  term of (29) is constructed using (43), such as:

$$\delta_1 = \delta_2 = \delta_3 = 0.0002 \quad (46)$$

If the piezo actuator is used, the panel vibration is damped in the inner loop. Then, the output can be chosen as  $y = \theta$ . This process is the same as the one used in the pervious section by choosing  $\alpha = 0$ . However, in the simulations, it is shown that output redefinition approach results in a better performance in active control, too.

## Singular Terminal Sliding Mode Controller Design

As mentioned, terminal sliding mode controllers are mainly used in controlling the systems of complex dynamics. In the complex dynamics, due to the lack of accurate information on the system, there exist some uncertainties in the modeled dynamics. A special feature of the terminal sliding mode controllers is their nature of being robust against uncertainties [23]. In order to simultaneously benefit from all terminal sliding mode controllers (like appropriate setting time and robustness to uncertainties) and to troubleshoot the significant standard terminal controller (system control around singular point(s)) in a simultaneous manner, the nonsingular terminal sliding mode controller is introduced [38].

Considering equation (12), the objective is to design an appropriate controller to converge the states  $X$  to the desired states  $X^d$ . Tracking the attitude angles  $\theta$  to the command trajectory  $\theta_d$  and damping panel deflection are the main objective here.

At first, it is assumed that no piezo is used as the actuator (equation (22)). Similar to the STA method, the new output is redefined as:  $y = \theta + \alpha q$ .

By borrowing  $X_1 = \theta + \alpha q$  and  $X_2 = \dot{\theta} + \alpha \dot{q}$ , from equation (32), we can write:

$$\begin{aligned} \dot{X} &= f_T(X) + g_T(X)u_T + d(t) \\ f_T &= f_S g_T = g_S \end{aligned} \quad (47)$$

The sliding surface is defined as:

$$s = e + \frac{1}{\beta} \dot{e}^{\frac{p}{q}} \quad (48)$$

where, the values  $p$  and  $q$  ( $p > q$ ) are both odd and positive values and  $\beta > 0$ . The nonsingular terminal sliding mode control rule is defined as:

$$u_T = -g_T^{-1}(x) \left[ f_T(x) + \beta \frac{q}{p} \dot{e}^{2-\frac{p}{q}} + (L + \eta) \text{sign}(S) \right] \quad (49)$$

where,  $\eta > 0$ ,  $1 < p/q < 2$  and the  $L$  value are obtained from (44).

$$|\dot{d}(X, t)| < L \quad (50)$$

For stability approval, (49) is obtained from Lyapunov theory. The Lyapunov function is chosen as:

$$V = \frac{1}{2} s^2 = \frac{1}{2} s^T s \quad (51)$$

For simplicity, in stability proof, the tracking is changed to the regular problem using axis transformation;

$$\begin{cases} e \rightarrow X_1 \\ \dot{e} \rightarrow X_2 \end{cases}$$

hence, error is replaced with states:  
The time derivative of the surface is equal to:

$$\dot{s} = \dot{X}_1 + \frac{1}{\beta} \frac{p}{q} X_2 \dot{X}_2 \quad (52)$$

According to the Eq. 52, where  $u_T$  and  $\dot{X}$  is are replaced in (52), we have:

$$\dot{s} = \frac{1}{\beta} \frac{p}{q} X_2^{\frac{p-1}{q}} (d(X, t) - (L + \eta) \text{sign}(s)) \quad (53)$$

Hence, we can write:

$$\dot{V} = s \dot{s} = \frac{1}{\beta} \frac{p}{q} X_2^{\frac{p-1}{q}} (sd(X, t) - (L + \eta) |s|) \quad (54)$$

According to  $X_2^{\frac{p-1}{q}} > 0$  when  $X_2 \neq 0$ , Eq.55 is yield as:

$$\begin{aligned} \dot{V} = s \dot{s} &\leq \frac{1}{\beta} \frac{p}{q} X_2^{\frac{p-1}{q}} (-\eta |s|) \\ &= -\frac{1}{\beta} \frac{p}{q} X_2^{\frac{p-1}{q}} \eta |s| = -\eta' |s| \end{aligned} \quad (55)$$

$$\eta' = \frac{1}{\beta} \frac{p}{q} X_2^{\frac{p-1}{q}} \eta > 0 \text{ when } X_2 \neq 0 \quad (56)$$

Hence, the stability is guaranteed and states approach zero in limited time.

According to Eqs. 45-46, the terminal gains are chosen as:

$$\begin{aligned} \beta &= [0.01 \quad 0.04 \quad 0.05], \eta = [0.1 \quad 0.1 \quad 0.1] \\ n = 1 \Rightarrow q = 3, p = 5 \Rightarrow \frac{p}{q} &= \frac{5}{3} \end{aligned} \quad (57)$$

## Simulation results

The simulation results for the closed loop system (12) with the control laws derived in the previous sections are obtained using MATLAB and SIMULINK software. In this simulation, the system parameters are chosen the same as those in [17]:  $E_b = 76 * 10^9 \text{ N/m}^2, \rho_b = 2840 \text{ kg/m}^3, l_b = 0.7 \text{ m}, b = 0.5 \text{ m}, t_b = 4 \text{ mm}, I_c = 4 \text{ kgm}^2, w_b = 50 \text{ mm}, E_p = 61 * 10^9 \text{ N/m}^2, \rho_p = 7400 \text{ kg/m}^3, l_p = 0.2 \text{ mm}, t_p = 0.75 \text{ mm}, d_p = 22 * 10^{-12} \text{ mV}^{-1}, w_p = 50$

The torque control input and its rate are bounded as:  $|\tau| < 0.8 \text{ N.m}$ ,  $|\dot{\tau}| < 0.8 \text{ N.m/s}$  and the electrodes voltage is bounded as:  $|v| < 1500 \text{ v}$ . The spacecraft disturbances are simulated according to Eq. 44.

The noise of the earth sensor is modeled through Gaussian distribution with its mean and standard deviation of 0 and 0.2 degrees, respectively. The noise of gyro sensor is modeled as:

$$\omega_M = H_{gyro} \omega + \omega_D + \omega_N$$

Where,  $\omega$  and  $\omega_M$  are the actual and measured angular velocities, respectively. Random drift noise  $\omega_D$  and random bias rate  $\omega_N$

are of Gaussian distribution, with  $10^{-6}$  rad/s standard deviation and zero mean, respectively. Gyro transfer function is:

$$H_{gyro} = \frac{4469s + 89.22}{s^3 + 89.22s^2 + 4469s + 89.22}$$

A number of time simulations are carried out and the designed controllers performances are tested. In all simulations, no damping term in the spacecraft equation is considered. All simulations are made in the large maneuver subject to combined uncertain conditions.

### Active and passive STA controllers

The results for the active (using reaction wheels as attitude actuator on the hub and piezoelectric patches as panel deflection actuator) and passive (using only reaction wheels as actuator) STA and terminal controllers are shown in Figs.3 and 4, respectively, where output redefinition method (ORM) in uncertain conditions is applied.

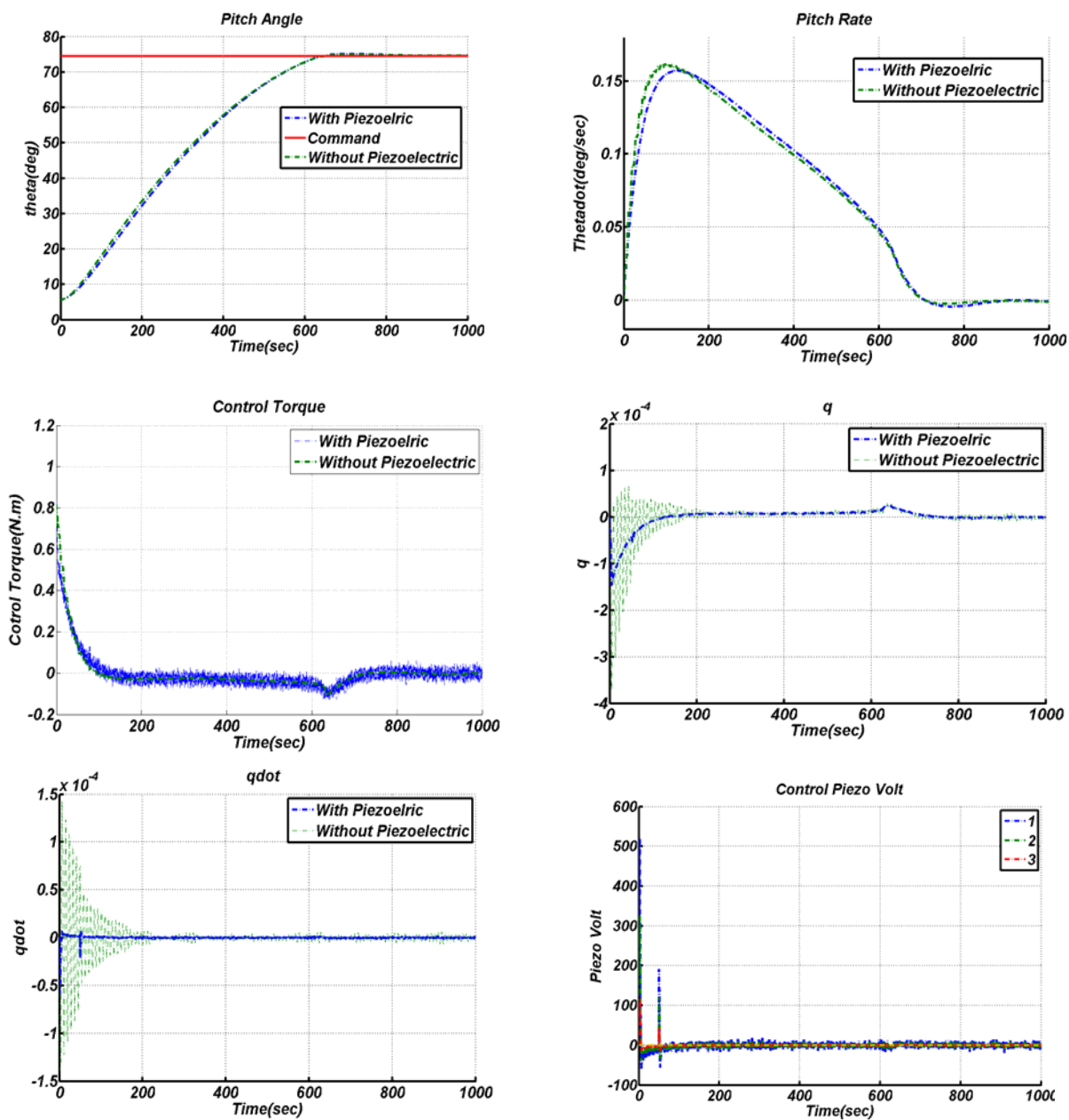


Figure 3. Active and passive super twisting controller: (a) spacecraft attitude, (b) angular velocity, (c) reaction



wheel torque, (d) tip deflection, (e) tip rate, and (f) control electrodes voltage.

### Active and passive singular terminal sliding mode controller

As observed in Figs.3a,b and 4a and b, using the piezo actuator has low effect on attitude performance, where the panel deflection is damped rapidly (Figs.3,4 d, and e) by using smaller controller effort (Figs.3 and 4c).

### Comparing the performance of the terminal sliding mode and STA controllers

Comparing the performance of the two designed controllers, the system responses are shown in Fig.5 in uncertain condition without using piezo patches and with an output-redefined method.

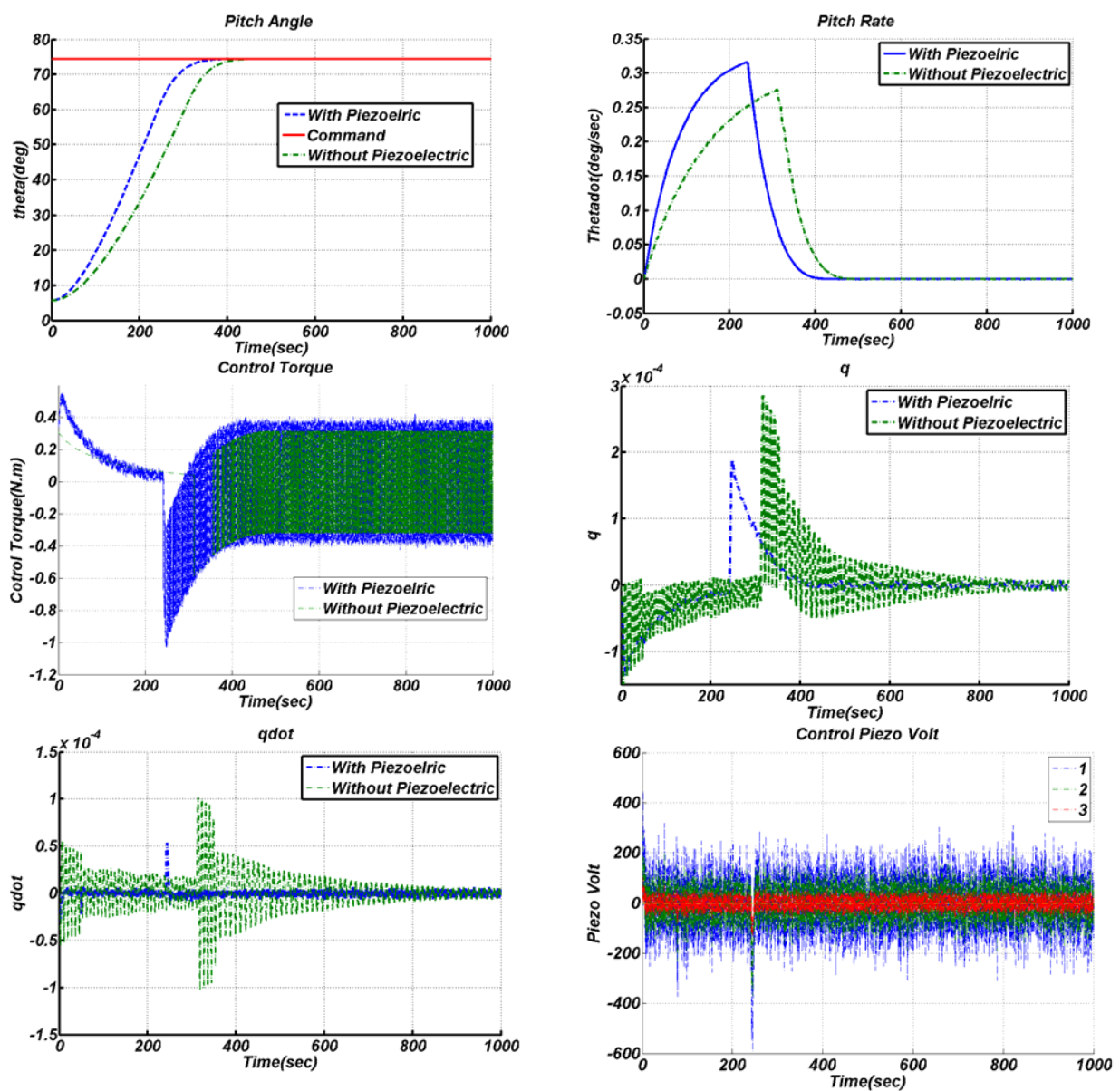


**Figure 4.** Terminal sliding mode controller with and without piezoelectric patches: (a) spacecraft attitude, (b) angular velocity, (c) reaction wheel torque, (d) tip deflection, (e) tip rate, and (f) electrode voltage.

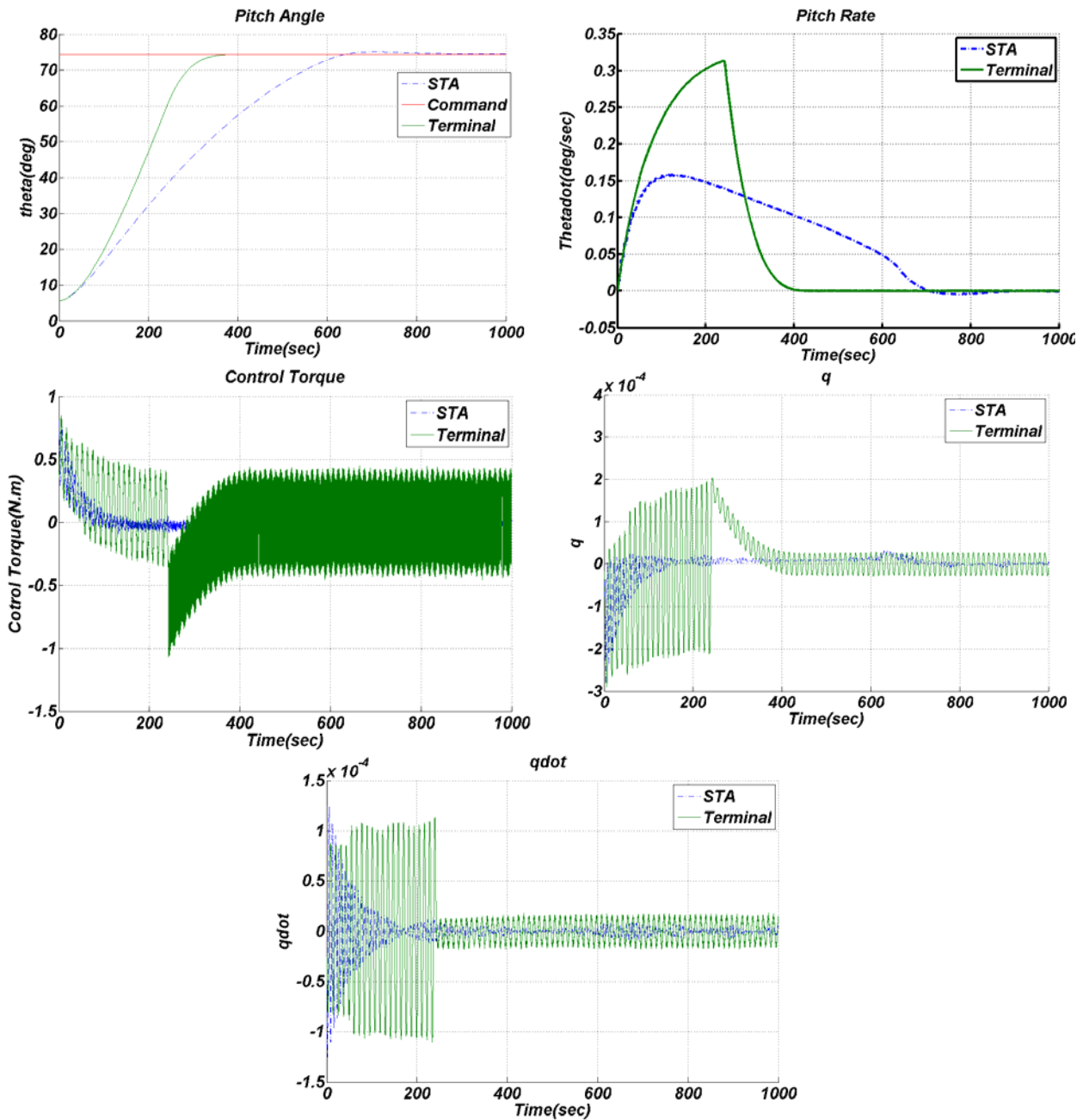


**Figure 5.** STA and Terminal Controller without using output redefinition approach and piezoelectric patches: (a) spacecraft attitude, (b) angular velocity, (c) reaction wheel torque, (d) tip deflection, and (e) tip rate.

As observed in Figs.5a and 5b, the terminal controller can track the desired trajectory in a smaller settling time (5a) and with a larger angular rate (5b), while the chattering is not removed (5c). Here, in STA, the chattering is removed (3c). As observed, in the terminal method, the panel deflection cannot be damped (5e and 5f) and STA has a better performance. It could be deduced that in the terminal methods, the chattering excites the panel vibration modes.

### Terminal sliding mode controller with and without using Output Redefined Method

Showing the output redefined method performance, the spacecraft response to terminal controller in both cases of with and without RDF are drawn in Fig.6. Here, by adapting this newly proposed method, settling time and controller

effort are reduced (6a) and (6c). In the terminal method, chattering exists, but using output redefinition method chattering begins after 400 sec with a smaller control effort. By adapting this

method, the panel deflection is reduced and can be damped better (6e, f).

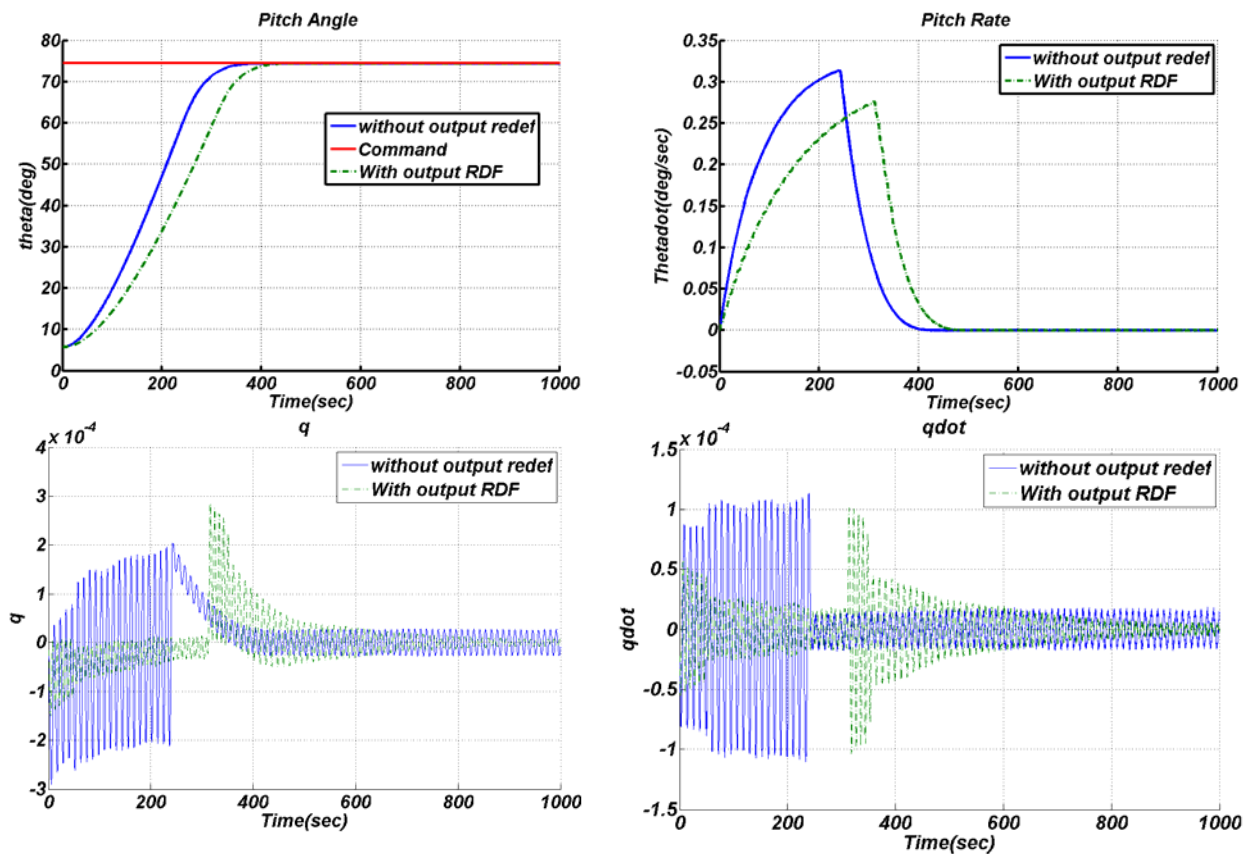


**Figure 6.** Terminal Controller with and without using output redefinition approach and no piezoelectric patches: (a) spacecraft attitude, (b) angular velocity, (c) reaction wheel torque, (d) tip deflection, (e) tip rate, and (f) control electrodes voltage.

In brief, the terminal controller has a better performance in the attitude response and a poor performance in the damping panel vibrations. By using the piezo electric patches as actuators, the chattering is reduced. The output redefinition approach improves the system performance.

## Conclusion

The active and passive control of the flexible spacecraft are presented. In passive controller, it is assumed that only one reaction wheel is obtained on the hub without using any actuator on the panel. In active controller, the controller is designed by applying an inner loop through piezoelectric as a sensor and actuator to reduce

the panel vibration and an outer loop to control the spacecraft attitude in large maneuver.

The flexible spacecraft is controlled by two outer controllers. One, a high order-sliding mode controller using super twisting algorithm and the other, a nonsingular terminal sliding mode controller. With respect to the non-minimum phase feature, the output redefinition approach is introduced.

The performances of these proposed controllers are compared in uncertain conditions. It is found that the terminal controller has a better performance in the attitude response against its performance in the damping panel vibrations. In STA, the chattering is almost removed; consequently, the damping panel vibration occurs in a short time.

Using the piezo electric patches as actuators caused more rapid damping of the vibrations and a smaller control effort. The output redefinition approach improved the system performance.

### Declaration of conflicting interests

The authors declare that there is no conflict of interest. Funding .The author received no financial support for the research, authorship, and/or publication of this article.

### References

- [1] Song Z, Li, H. and Sun, K.. "Finite-Time Control for Nonlinear Spacecraft Attitude Based on Terminal Sliding Mode Technique," *ISA Transactions*, Vol. 53, 2014, pp.117–124.
- [2] Zhu, Z., Xia, Y. and Fu, M., "Adaptive Sliding Mode Control for Attitude Stabilization with Actuator Saturation," *IEEE Trans Indus Elect*, Vol. 58, 2011, p. 10.
- [3] Hu, Q., "Sliding Mode Attitude Control with L<sub>2</sub>-gain Performance and Vibration Reduction of Flexible Spacecraft with Actuator Dynamics," *Acta Astronautica*, Vol. 67, 2010, pp. 572–583.
- [4] Liu, H., Guo, L. and Zhang, Y., "An Anti-Disturbance PD Control Scheme for Attitude Control and Stabilization of Flexible Spacecraft," *Nonlinear Dynamics*, Vol. 67, 2012, pp. 2081–2088.
- [5] Pukdeboon, Ch. "Optimal Output Feedback Controllers for Spacecraft Attitude Tracking," *Asian J Control*, Vol. 15, No. 4, 2013, pp. 1–11.
- [6] Fridman, L. and Shtessel, Y., "Edwards C and Yan XG. Higher-Order Sliding-Mode Observer for State Estimation and Input Reconstruction in Nonlinear Systems," *I J Robust Nonlinear Control* Vol. 18, No. 4-5, 2008, pp. 399–412.
- [7] Zhou, Y., Soh Y.C. and Shen, J. X., "High-Gain Observer with Higher-Order Sliding Mode for State and Unknown Disturbance Estimations," *I J Robust Nonlinear Control*, Vol. 24, No. 15, 2013, pp. 2136- 2151.
- [8] Zhu, F. and Yang, J. "Fault detection and Isolation Design for Uncertain Nonlinear Systems Based on Full-Order Reduced-Order and High-Order High-Gain Sliding-Mode Observers," *I J Control*, Vol. 86, No. 10, 2013, pp. 800–1812.
- [9] Rios, H., Davila, J. and Fridman, L., "High-Order Sliding Mode Observers for Nonlinear Autonomous Switched Systems with Unknown Inputs," *J Franklin Inst*, Vol. 349, No. 10, 2012, pp. 2975–3002.
- [10] Kermani, M.R., Moalem, M. and Patel, R.V., *Applied Vibration Suppression using Piezoelectric Materials*. Nova Science Publishers 2008.
- [11] Song, G. and Kotejoshyer, B., "Vibration Reduction of Flexible Structures During Slew Operations," *International Journal of Acoustics and Vibration*, Vol. 7, No. 2, 2002, pp. 105–109.
- [12] Shan, J.J., Liu, H.T. and Sun, D. Slewing and Vibration Control of a Single-Link Flexible Manipulator by Positive Position Feedback. *Mechatronics*, Vol. 15, No. 4, 2005, pp. 487–503.
- [13] Jiang, J.P. and Li, D.X., "Robust H<sub>∞</sub> Vibration Control for Smart Solar Array Structure," *Journal of Vibration and Control*, 2010, Vol. 17, No. 4, pp. 505-515.
- [14] Mahmoodi, S.N., Ahmadian, M. and Inmari, D.J., "Adaptive Modified Positive Position Feedback for Active Vibration Control of Structures," *Journal of Intelligent Material Systems and Structures*, Vol. 21, 2010, pp. 571-580.
- [15] Fey, R.H.B., Wouters, R.M.T. and Nijmeijer, H., "Proportional and Derivative Control for Steady-State Vibration Mitigation in a Piecewise Linear Beam System," *Nonlinear Dynamic*, Vol. 60, 2010, pp. 535-549.
- [16] Ding, S. and Zheng, W.X. "Non Smooth Attitude Stabilization of a Flexible Spacecraft," *IEEE Transactions on Aerospace and Electronic Systems*, Vol. 50, No. 2, 2014, pp. 1163-1183.
- [17] Azadi, M., Fazelzadeh, S.A., Eghtesad, M. and Azadi, E., "Vibration Suppression of Smart Nonlinear Flexible Appendages of a Rotating Satellite by using Hybrid Adaptive Sliding Mode/ Lyapunov Control," *Journal of Vibration Control*, Vol 19, Issue 7, 2013, pp. 975-991.
- [18] Meyer, J.L., Harrington, W.B., Agrawil, B. N. and Song, G., Vibration Suppuration of a Spacecraft Flexible Appendage Using Smart Material Smart Material, *Smart Mater Structure*, Vol. 7, No. 95, 1998, pp.95-104.
- [19] Hu, Q., "Sliding Mode Attitude Control with L<sub>2</sub>-Gain Performance and Vibration Reduction of Flexible Spacecraft with Actuator Dynamics," *Acta Astronautica*, Vol. 67, 2010, pp. 572-583.
- [20] Malekzadeh, M., Naghash, A. and Talebi, H.A., Robust Attitude and Vibration Control of a Nonlinear Flexible Spacecraft, *Asian Journal of Control*, 14, No. 2, 2012, pp. 553-563.
- [21] Derafa, L., Benallegue, A. and Fridman, L., Super Twisting Control Algorithm for the Attitude Tracking of a Four Rotors UAV," *J Franklin Inst*, Vol. 349, 2012, pp. 685-699.
- [22] Moreno, J.A., A Linear Framework for the Robust Stability of a Generalized Super-Twisting Algorithm," *Proceedings of Sixth IEEE Conference on Electrical Engineering Computing Science and Automatic Control (CCE 2009)*, 2009, pp. 1-6.
- [23] Jinkun, L. and Xinhua, W., *Advanced Sliding Mode Control for Mechanical Systems: Design, Analysis and MATLAB Simulation (1<sup>st</sup> edn)*, Tsinghua University Press, Beijing and Springer-Verlag Berlin Heidelberg 2012.